Improvement in Flow Distribution for Effective Thermal Management in Thermoelectric Generator for Waste Heat Recovery

Chander Veer, Shobhana Singh, and Jasa Ram

Abstract In an automobile, only one-third of the total fuel energy is used for propulsion, and the remaining two-third is lost to engine coolant and the exhaust as waste. Thermoelectric generators (TEG) demonstrate huge potential in automotive applications by recovering the exhaust waste heat and converting it into direct electric power. TEG helps escalate the engine's fuel efficiency. However, extracting waste heat from automobile exhaust using TEG manifests practical difficulties attributed to thermoelectric materials, design, and operating conditions. Ineffective configurations and heat exchanger designs lead to non-uniform flow and temperature distribution on the hot and cold sides of TEG, causing undesirable power output, which lowers the entire system's efficiency. In this study, the flow distribution of exhaust gas through the automotive TEG with pin fin heat exchanger is simulated using Computational Fluid Dynamics (CFD). Improvement in the flow pattern using passive flow distributors such as guide vanes at different angles is analyzed to attain the temperature uniformity through the hot heat exchanger surface. A detailed analysis of flow distribution and its influence on the local and average temperature distribution is presented. Results provide critical design recommendations to improve the flow distribution in an automotive TEG for exhaust waste energy recovery.

Keywords Thermoelectric generator · Heat exchanger · Flow distribution · Temperature uniformity · Computational fluid dynamics

Nomenclature

h	Specific enthalpy (J/kg K)
k	Thermal conductivity (W/m K)

C. Veer · S. Singh (✉)
Indian Institute of Technology Jodhpur, Jodhpur, Rajasthan 342037, India
e-mail: shobhana@iitj.ac.in

J. Ram
Defense Laboratory Jodhpur, Jodhpur, Rajasthan 342011, India

R. K. Tyagi et al. (eds.), *Advances in Engineering Materials*, Lecture Notes in Mechanical Engineering,https://doi.org/10.1007/978-981-99-4758-4_2

$\boldsymbol{k}'$	Turbulent kinetic energy (J/kg)
p	Pressure (Pa)
u, v, w	Velocities (m/s) in x, y, and z directions respectively
$\boldsymbol{V}$	Velocity vector (m/s)

Greek Symbols

ρ	Density (kg/m^3)
θ	Temperature (K)
$\boldsymbol{\omega}'$	Specific rate of dissipation of turbulent kinetic energy (1/s)
μ	Dynamic viscosity (Pa s)

Subscripts

x, y, z	Directions corresponding to Cartesian coordinates

1 Introduction

The transportation sector alone accounts for 55% of the total fossil fuel usage, and this consumption is increasing at an annual rate of 1.4% [1]. Increasing fossil fuel consumption and demand has raised significant concerns regarding the sustainability of natural resources and petroleum products. Many avenues can be explored to reduce energy consumption, and improving the fuel efficiency of automobiles is one of them. For a typical automobile engine, 40% of the fuel energy is wasted in the form of exhaust [2]. Recovering this waste heat can significantly improve fuel efficiency and reduce harmful emissions. Thermoelectric generators have proven to be a promising device in waste heat recovery from automobile exhaust, which can directly convert the exhaust waste heat into useful electrical energy using the Seebeck effect. In order to achieve a high power output from the Automotive Exhaust Thermoelectric Generator (AETEG), a high temperature on the hot side of the Thermoelectric (TE) is needed. This necessitates the design of an efficient heat exchanger, which can extract the maximum heat from the exhaust air and maintain a uniform temperature over the heat exchanger surface. For AETEG, the most decisive factors that affect its performance are the temperature and flow distribution.

To achieve a uniform and high temperature on the surface of the heat exchanger, several heat exchanger designs have been studied. Kumar et al. [3] tested three heat exchanger configurations, namely triangular, rectangular, and hexagonal. The

author concluded that a rectangular heat exchanger exhibits a more balanced performance among the three. In addition to the hot heat exchanger's shape, the hot heat exchanger's internal geometry is an essential criterion in AETEG application. A flat-shaped heat exchanger with three different internal configurations, i.e., accordion, fishbone, and scattered was investigated by Su et al. [4]. The author concluded that an accordion-shaped heat exchanger is best suited for the application in AETEG.

Improving airflow distribution can significantly improve the temperature distribution over the heat exchanger surface. Nagesh et al. [5] conducted an experimental study to evaluate the thermal performance of AETEG using the flow straighteners with varying porosity at different locations. It is inferred from their study that by placing the flow straightener having a porosity of 0.4–0.5 in the middle of the exhaust channel, the power output is maximized. There is a scarcity of literature that address the problem of flow maldistribution. The focus of the present study is to improve the flow distribution inside a pin fin heat exchanger using guide vanes. Guide vanes at three different angles are placed at the inlet diffuser section, and their effect on the thermal–hydraulic performance of the heat exchanger and temperature uniformity over the heat exchanger surface is studied.

2 Physical Model

Figure 1a depicts the physical model of AETEG. The heat exchanger has a cross section area of 200 mm × 100 mm and a length of 250 mm. Circular pin fins of diameter 10 mm and length of 100 mm are used inside the heat exchanger, keeping the volume of pin fins 1/10th to that of the heat exchanger volume. Air with temperature-dependent properties is used as the working fluid (see Table 1). The inlet and outlet diffuser, hot heat exchanger, and heat sink material are taken as aluminum. Bismuth telluride is taken as the thermoelectric material, and for insulation, asbestos is selected. All material properties are listed in Table 2.

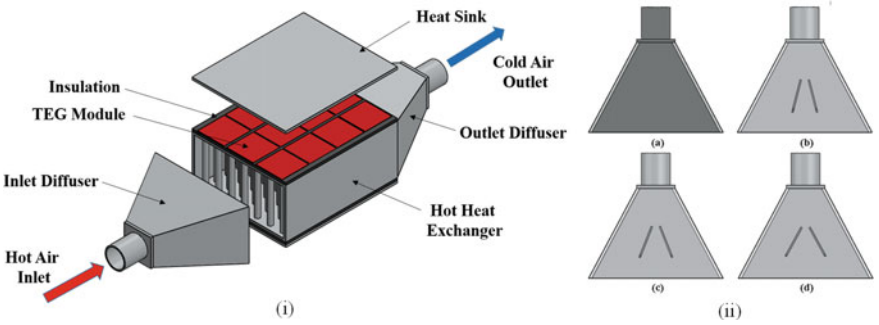

Fig. 1 Physical model of AETEG (i) Components of AETEG (ii) inlet diffuser **a** without guide vanes and guide vanes at different angles **b** 30° **c** 45° **d** 60°

Table 1 Thermophysical properties of air

Property	Expression
Density (kg/m^3)	$3.7771 - 1.5884 \times 10^{-2}\,\theta + 3.3564 \times 10^{-5}\,\theta^2 - 3.7685 \times 10^{-8}\,\theta^3 + 2.1407 \times 10^{-11}\,\theta^4 - 4.8308 \times 10^{-15}\,\theta^5$
Specific heat capacity (J/kg K)	$1013.1890 + 0.2336\,\theta - 2.3511 \times 10^{-3}\,\theta^2 + 7.3109 \times 10^{-6}\,\theta^3 - 9.2297 \times 10^{-9}\,\theta^4 + 5.3424 \times 10^{-12}\,\theta^5 - 1.1797\,10^{-15}\,\theta^6$
Thermal conductivity (W/m K)	$1.0132 \times 10^{-3} + 9.0445 \times 10^{-5}\,\theta - 2.9040 \times 10^{-8}\,\theta^2 + 4.6490 \times 10^{-12}\,\theta^3$
Dynamic viscosity (Pa s)	$2.7545 \times 10^{-6} + 6.1156 \times 10^{-8}\,\theta - 3.0361 \times 10^{-11}\,\theta^2 + 8 \times 10^{-15}\,\theta^3$

Table 2 Thermophysical properties of aluminum, asbestos, and bismuth telluride

Material	Density (kg/m^3)	Specific heat capacity (J/kg K)	Thermal conductivity (W/m K)
Aluminum	2719	871	202
Asbestos	2400	566	0.15
Bismuth telluride	7500	544	1.5

TE module has a cross section of 60 mm × 60 mm and a height of 5 mm. A diffuser section is provided before the hot heat exchanger to distribute the flow before reaching the inlet heat exchanger. The diffuser has a length of 140 mm, and the cross section expands from 50 mm × 50 mm to 200 mm × 100 mm.

For this study, guide vanes at three different angles (30°, 45°, and 60°) are placed in the inlet diffuser section, as shown in Fig. 1b. The performance of the heat exchanger has been evaluated based on different thermal–hydraulic parameters such as flow streamlines, temperature uniformity index, and power output from the thermoelectric modules.

3 Numerical Model

A three-dimensional CFD model is studied to analyze the effect of guide vanes at different angles on flow and heat transfer behavior. Only half of the geometry is simulated to simplify the model and solution process, and symmetry boundary condition is imposed on the symmetric plane.

The following assumptions have been taken into account while solving the numerical model,

1. The airflow is steady, incompressible, and turbulent.
2. Radiation heat transfer is neglected.
3. Perfect thermal contact between contact surfaces such that the contact resistance is neglected.

Using the above assumptions, the governing equations are reduced to the form, Continuity equation,

$$\nabla \cdot (\rho \boldsymbol{V}) = \boldsymbol{0} \tag{1}$$

Momentum equation,

$$\nabla(\rho u \boldsymbol{V}) = -\nabla p_x + \mu \nabla^2 u \tag{2}$$

$$\nabla(\rho v \boldsymbol{V}) = -\nabla p_y + \mu \nabla^2 v \tag{3}$$

$$\nabla(\rho w \boldsymbol{V}) = -\nabla p_z + \mu \nabla^2 w \tag{4}$$

Energy equation,

$$\nabla(k \nabla \theta) = \nabla(\rho h \boldsymbol{V}) \tag{5}$$

SST k-ω model,

$$\nabla.\left(\rho \boldsymbol{V} \boldsymbol{k}'\right) = \nabla.\left[\rho \nabla \boldsymbol{k}'(\mu + \sigma_{k'1}\mu_t)\right] + \rho(P_k - \in) \tag{6}$$

$$\nabla.\left(\rho \boldsymbol{V} \boldsymbol{\omega}'\right) = \rho \boldsymbol{\omega}'\left(\frac{\gamma P_k}{k'} - \beta\omega\right) + 2(1 - F_1)\left(\frac{\rho\sigma_{\omega'2}}{\omega'}\right)\nabla \boldsymbol{k}' \nabla \boldsymbol{\omega}' + \nabla.\left[\rho \nabla \boldsymbol{\omega}'(\mu + \sigma_{\omega'1}\mu_t)\right] \tag{7}$$

where $\sigma_{k'1} = 0.5$, $\sigma_{k'2} = 0.5$, $\sigma_{\omega'1} = 0.5$, $\sigma_{\omega'2} = 0.856$, $\beta_1 = 0.075$, $\beta_2 = 0.0828$ [6].

Following are the boundary conditions that are imposed on the CFD model: Inlet velocity of exhaust air is set to 6.5 m/s and inlet temperature as 473 K. The Reynolds number at the inlet is 23,965 and flow is in a turbulent region. At the outlet, pressure outlet condition is used with a gauge pressure value set to 0 Pa. To have a perfect thermal contact at every interface, the coupled wall boundary condition is used. A constant wall temperature condition with a temperature of 298 K is employed on the heat sink. All surfaces exposed to ambient have an insulated boundary condition with the heat flux value set to 0 W/m^2.

The numerical model of AETEG is solved using ANSYS Fluent 2020R2. SST k-ω model is employed to simulate the turbulent flow of exhaust air. To achieve the pressure–velocity coupling, the COUPLED scheme is used. The gradients are calculated using the Least Square Cell-Based method, and pressure is discretized using the PRESTO scheme. To conserve the energy, turbulent kinetic energy, specific dissipation rate, and momentum equation, the second-order upwind scheme is used. The convergence criteria are set to 10^{-3} for continuity and 10^{-6} for k', ω', momentum equation, and energy equation.

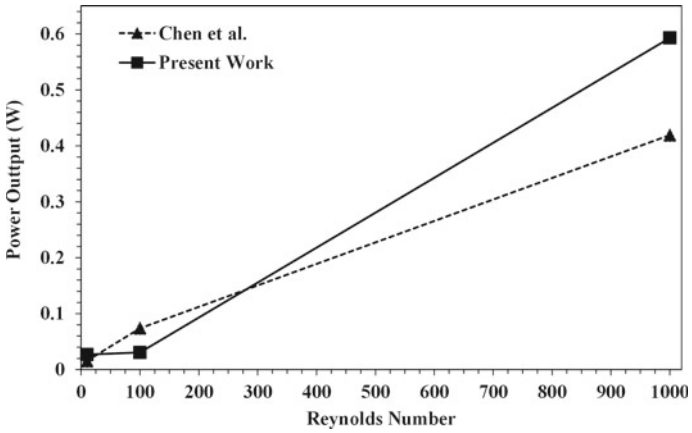

Fig. 2 Numerical validation between the present work and the work reported by Chen et al.

For the model's accuracy, a mesh independence study is performed with number of elements from 43,909 to 24,61,819. The air outlet temperature and pressure drop converged as the mesh size increased. To balance accuracy and computational time, a grid size of 2.5 mm is selected with the number of elements 12,75,373.

The numerical model discussed in the present research is validated by a study reported by Chen et al. [7]. The average surface temperature on the cold side and hot side of TE modules is compared. It is observed that the variation between the present numerical model and the previously reported study is less than 2%.

The numerical validation is also performed with respect to the power output from the TEG. The performance parameter comparison between the present study and the analysis conducted by Chen et al. [7] is shown in Fig. 2.

4 Results and Discussion

Using the solution methodology described above, the model is numerically investigated to study the effect of guide vanes placed at three different angles on the thermal–hydraulic performance of the hot heat exchanger. Keeping in mind the goal of temperature uniformity over the heat exchanger surface, the performance of the hot heat exchanger is analyzed with the temperature uniformity index (γ) [8], which can be defined as,

$$\gamma = 1 - \frac{1}{n} \sum_{j=1}^{n} \frac{\theta_j - \theta_{\text{avg}}}{\theta_{\text{avg}}} \tag{8}$$

Here, n is the total number of modules, θ_j is the average temperature of the jth module (K), and θ_{avg} is the average temperature of the heat exchanger surface (K).

One important parameter to judge the performance of AETEG is the power output from the modules. For simplicity, the electrical simulations have not been included in the present study, and theoretical power output has been calculated based on the following equation,

$$\text{Power Output} = n\frac{\alpha^2 \Delta\theta^2}{4R} \tag{9}$$

Here, n is the number of modules, α is the Seebeck coefficient (V/K), $\Delta\theta$ is the temperature difference across a single module (K), and R is the electrical resistance of the module (ohm). For simplicity, the results are represented as Case 1—Without any guide vanes, Case 2—Guide Vanes at 30°, Case 3—Guide Vanes at 45°, and Case 4—Guide Vanes at 60°.

4.1 Flow Analysis

The velocity streamlines on the symmetric plane of the hot heat exchanger are shown in Fig. 3. From the streamlines flow on the symmetry plane, it can be concluded that if no guide vanes are present, the flow is going straight from inlet to outlet, and no airflow is occurring near sidewalls. The vortices forming due to flow separation by fins are also limited to the middle portion of the hot heat exchanger. However, as soon as the guide vanes are inserted in the inlet diffuser, a change in the flow pattern of exhaust air is observed. As we start to increase the angle of guide vanes, more and more air is deflected toward the sidewalls of the hot heat exchanger. With the use of guide vanes, an increase in vortices can also be observed. Also, these vortices are not limited to the middle portion. Instead, they are distributed in the whole hot heat exchanger.

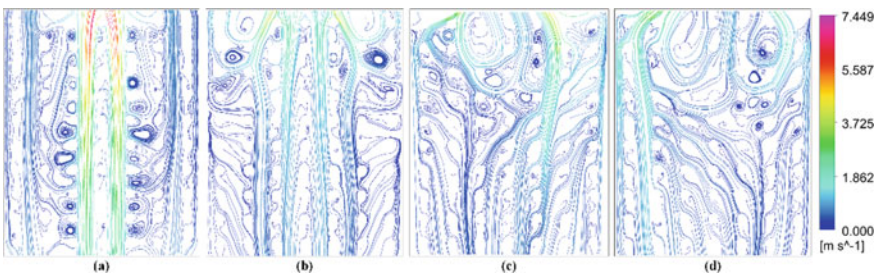

Fig. 3 Flow streamlines on the symmetric plane of hot heat exchanger **a** case 1 **b** case 2 **c** case 3 **d** case 4

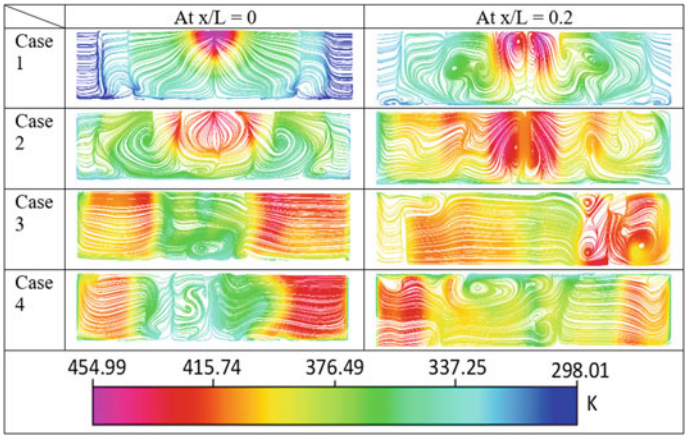

Fig. 4 Flow streamlines on transverse planes of hot heat exchanger drawn at two different locations

Figure 4 represents the streamlines on two transverse planes, one at the hot heat exchanger inlet and the second after two rows of pin fins. In the table, x represents the distance from the heat exchanger inlet, and L represents the total heat exchanger length. The color code represents the temperature of exhaust air. It is inferred that, for the case 1, most part of the hot air is going straight from inlet to the outlet diffuser and that too through the middle part of heat exchanger. There is no direct contact between the hot air and the heat exchanger surface. So most of the heat transfer to the heat exchanger surface is by conduction through pin fins.

However, when guide vanes are present, hot air is also deflected toward the bottom surface of the heat exchanger. Now the heat is transferred to the surface by conduction through fins as well as the direct contact of air, resulting in a high heat transfer rate and higher surface temperature. At an angle of 30^{o} (case 2), most of the hot air flow is still through the middle portion of the heat exchanger. However, if the angle is increased to 60^{o} (case 4), the flow is more directed toward the sidewalls of the hot heat exchanger. Guide vanes kept at an angle of 45^{o} (case 3), present a more balanced flow than the other two resulting in a more uniform distribution of hot air throughout the hot heat exchanger.

4.2 Thermal Analysis

The variation in average surface temperature of hot heat exchangers along the length is shown in Fig. 5. The abscissa represents the normalized heat exchanger length and the ordinate represents the normalized surface temperature of hot heat exchanger with respect to the air inlet temperature. In comparison with the base case, i.e., no guide vanes, there is an increase of about 5–7% in the average surface temperature

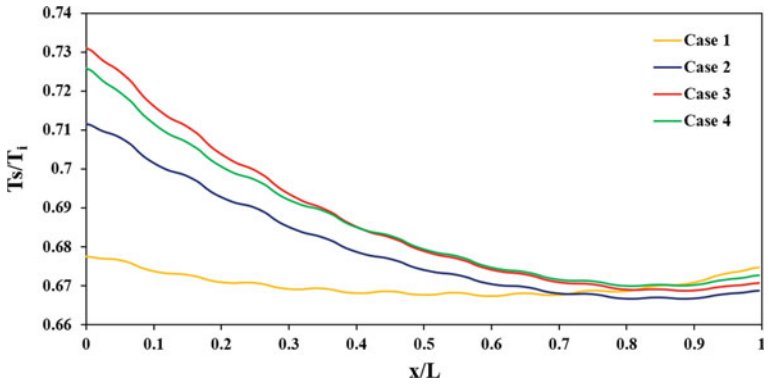

Fig. 5 Variation of surface temperature along the length of the hot heat exchanger

at the heat exchanger inlet. This increase in surface temperature is highest for case 3 and lowest for case 2.

These results are also in-line with the flow distribution of exhaust gas, in which it is observed that flow was more uniform in case 3 as compared to case 2 and case 4. This increase in surface temperature is attributed to the fact that with the use of guide vanes, the flow gets deflected toward a larger area of hot heat exchanger, and more and more hot air gets in contact with the hot heat exchanger, resulting in a higher heat transfer rate. Moving along the length of heat exchanger, a temperature gradient is observed on the heat exchanger surface. This temperature gradient is steeper for cases 2, 3, and 4, because the air is more distributed at the inlet of the hot heat exchanger. Further, the air temperature reduces along the length due to the continuous exchange of heat thereby reducing the exergy of air. This results in a low heat transfer rate near the hot heat exchanger outlet and consequently a low temperature on the surface.

4.3 Temperature Uniformity Index and Power Output

One of the goals in designing a heat exchanger for AETEG is to obtain a uniform temperature distribution over the surface. To have an idea of temperature uniformity in all cases, the temperature uniformity index is calculated and the results are given in Table 3. The results suggest that using guide vanes reduces the temperature uniformity over the surface. This is observed because the air is deflected toward a larger area at the heat exchanger inlet, resulting in increased heat transfer and a high surface temperature at the heat exchanger inlet.

Table 3 represents the maximum rated power output that is obtained from the AETEG. It can be seen that there is an increase of 58%, 113%, and 101% in power output from AETEG for cases 2, 3, and 4, respectively. This is due to the fact that the modules that are present near the inlet position of the hot heat exchanger are subjected to a much higher temperature difference than the case with no guide vanes.

Table 3 Performance parameters of heat exchanger for AETEG

Case	Case 1 (without guide vanes)	Case 2 (guide vanes at 30°)	Case 3 (guide vanes at 45°)	Case 4 (guide vanes at 60°)
Temperature uniformity index	0.991	0.976	0.967	0.971
Power output (W)	5.714	9.068	12.171	11.535

Also, the temperature near the outlet of the hot heat exchanger for cases 2, 3, and 4 is comparable to case 1, hence the modules which are present at the rear end of the hot heat exchanger generated power equivalent to case 1. The overall outcome is that the design with the guide vanes performs better in terms of power output than the design without guide vanes.

5 Conclusion

In this study, the effect of guide vanes placed inside the inlet diffuser at three different angles (30°, 45°, and 60°) on the flow and heat transfer behavior of exhaust gas is analyzed. The power output and temperature uniformity index are calculated for all four cases. It is concluded that there is a significant change in the performance of AETEG when the guide vanes are used. Following are the concluding remarks based on the present study:

1. The guide vanes significantly improve the flow distribution of hot air and the surface temperature of the hot heat exchanger.
2. The theoretical power output of AETEG is increased by 113%, with the guide vanes at an angle of 45°.
3. The design with no guide vanes present a higher value of temperature uniformity index, but when it comes to the overall performance, guide vanes perform better in terms of surface temperature and power output.

Acknowledgements Present work is carried out in collaboration with Defense Research Laboratory, Jodhpur under the research project (Project Number-S/DRDO/SHS/20210056).

References

1. González-Montaña JR, Alonso Diez AJ, Alonso de la Varga ME, Avila Téllez S (2016) "Por Determinar," Internacional de Ovinocultura. Asociación mexicana de especialistas en ovinocultura (AMTEO) 2016:127–137
2. Khan MQ, Malarmannan S, Manikandaraja G (2018) Power generation from waste heat of vehicle exhaust using thermoelectric generator: a review. IOP Conf Ser Mater Sci Eng 402(1). https://doi.org/10.1088/1757-899X/402/1/012174

3. Kumar CR, Sonthalia A, Goel R (2011) Experimental study on waste heat recovery from an internal combustion engine using thermoelectric technology. Therm Sci 15(4):1011–1022. https://doi.org/10.2298/TSCI100518053K
4. Su CQ, Wang WS, Liu X, Deng YD (2014) Simulation and experimental study on thermal optimization of the heat exchanger for automotive exhaust-based thermoelectric generators. Case Stud Therm Eng 4:85–91. https://doi.org/10.1016/j.csite.2014.06.002
5. Negash AA, Choi Y, Kim TY (2021) Experimental investigation of optimal location of flow straightener from the aspects of power output and pressure drop characteristics of a thermoelectric generator. Energy 219:119565. https://doi.org/10.1016/j.energy.2020.119565
6. Menter FR (1994) Two-equation eddy-viscosity turbulence models for engineering applications. AIAA J 32(8):1598–1605. https://doi.org/10.2514/3.12149
7. Chen WH, Lin YX, Bin Chiou Y, Lin YL, Wang XD (2020) A computational fluid dynamics (CFD) approach of thermoelectric generator (TEG) for power generation. Appl Therm Eng 173:115203. https://doi.org/10.1016/j.applthermaleng.2020.115203
8. Su CQ, Huang C, Deng YD, Wang YP, Chu PQ, Zheng SJ (2016) Simulation and optimization of the heat exchanger for automotive exhaust-based thermoelectric generators. J Electron Mater 45(3):1464–1472. https://doi.org/10.1007/s11664-015-4077-x